

Optimum suspension unit design for enhancing the mobility of wheeled armored vehicles[†]

Eun-Ho Choi¹, Jae-Bong Ryoo¹, Jin-Rae Cho^{2,3} and O-Kaung Lim^{2,*}

¹Division of Mechanical Systems Design, Pusan National University, Busan, 609-735, Korea

²School of Mechanical Engineering, Pusan National University, Busan, 609-735, Korea

³Research and Development Institute of Midas IT Co. Ltd., Gyeonggi-Do 462-807, Korea

(Manuscript Received February 4, 2009; Revised August 19, 2009; Accepted September 24, 2009)

Abstract

At the concept design stage of an armored vehicle, most design effects focus on firing accuracy, mobility and physical properties of the vehicle which are directly related to the firing power. This paper addresses an optimal design of the suspension unit of a four-wheeled armored vehicle to maximize the mobility performance after firing, which is characterized by the stabilizing time and the vertical acceleration of the driver's seat after firing. For the numerical analysis and design, a half-car dynamic model consisting of four degrees and four design variables, spring and damping coefficients of suspension and tire is constructed. The response surface functions (RSFs) of both the stabilizing time and vertical acceleration are approximated through the dynamic analysis of the four-degree half-car model. The objective function is defined by a weighted linear combination of the stabilizing time and the vertical acceleration, and the resulting optimization of the vehicle mobility is carried out by the PLBA algorithm. To support the validity of the proposed optimization procedure, illustrative numerical experiments are also performed.

Keywords: Wheeled armored vehicle; Mobility; Stabilizing time; Vertical acceleration; Response surface method; Design of experiments; PLBA algorithm

1. Introduction

The armored vehicle has been a key weapon in the ground warfare, thanks to its excellent off-road mobility and relatively long firing distance. As depicted in Fig. 1, armored vehicles are classified into two major types according to the traction mechanism, tracked and wheeled [1]. But, regardless of the traction type, the most important performance is a firing accuracy. The comparison between two types may be referred to Wong and Huang [2].

Regardless of the traction type, armored vehicles are not only being driven off-road but subjected to high firing impulse. In view of the requirement of high firing accuracy, these driving and impulsive conditions have been troublesome difficulties that should be resolved, particularly the suspension unit [3-6].

Since the early 2000's, modeling and simulation (M&S) technologies have been applied to the development process of a variety of weapon systems, and this trend is expected to be rapidly expanded to all countries in the world. Regarding ar-

mored vehicle, advanced countries such as the United States, Great Britain, France and Germany are intensively developing M&S frameworks, in order to flexibly respond to the changes in both the warfare environment and rapid advances in weapon development [7-11].

In accordance with such a worldwide trend, the government and academia in Korea, on their part, have struggled to settle down the basic technologies, founding specialized M&S centers, such as a simulation based acquisition (SBA). However, differing from the air and ship weapon systems, the evaluation and design technologies for ground weapons like armored vehicles have not been sufficiently established yet. The reason is because the major performances of both the systems and components of ground weapons have been traditionally designed simply along the standards of advanced countries, except for few opportunities for designing only few subsidiary components.

More recently, however, there has been an increasing need in Korea for deducing the required operational capability (ROC) of new weapon systems which can successfully meet the various battle environments in the future. Also, the demands for evaluating whether the existing weapon systems can provide the advanced performances which are expected to be needed in future are increasing. These demands on the

[†] This paper was recommended for publication in revised form by Associate Editor Jeong Sam Han

*Corresponding author. Tel.: +82 51 510 2306, Fax.: +82 51 512 9835

E-mail address: oklim@pusan.ac.kr

© KSME & Springer 2010

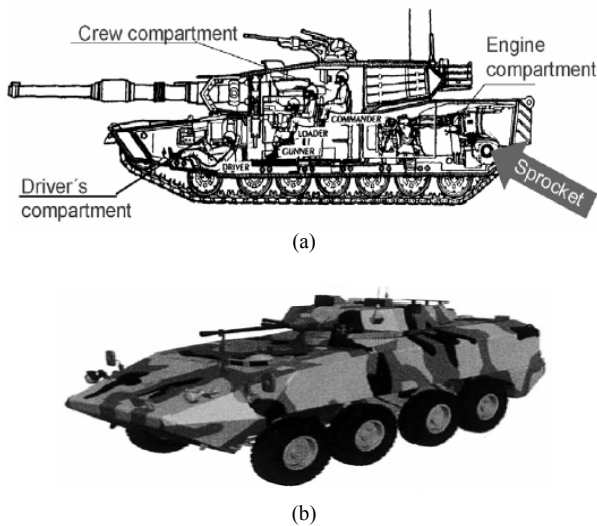


Fig. 1. Armored vehicle [2]: (a) tracked and (b) wheeled.

weapon engineering and science field in Korea naturally require numerical techniques for the performance evaluation and the concept design of comprehensive weapon systems.

In connection with the current situation in Korea, the present study intends to explore the applicability of the numerical optimization method for evaluating the dynamic responses of wheeled armored vehicles and for designing the suspension unit. The target dynamic responses are chosen as the stabilizing time and the vertical acceleration of a four-wheeled armored vehicle, and those are approximated by using response surface method (RSM) [12, 13] incorporated with design of experiments (DOE) [13]. And the corresponding design parameters are set by the spring and damping coefficients of the suspension unit and tire. The objective function is defined as a weighted linear combination of the stabilizing time and the vertical acceleration of the vehicle. The optimization problem is solved by PLBA optimization algorithm [14] which was developed based on the recursive quadratic programming.

2. Problem description

2.1 MOE analysis of ground weapon

Before commencing the development of a ground weapon like a wheeled armored vehicle, various virtual simulations for the war game scenarios, under expected conditions and Army Weapon Effectiveness Analysis Model (AWAM) [15], should be ahead to evaluate the measures of effectiveness (MOE) and the ROC. A number of input data such as geometry dimensions, material and mechanical parameters, and initial and boundary conditions should be input for the virtual simulations. These input data not only affect the accuracy of the MOE analysis results but exhibit the interactive relations, so that the reliability of both the design parameters and the correlation between design parameters is extremely important. Table 1 represents an illustrative example of the correlation.

Table 1. Illustrative correlation between design parameters and performances of a ground weapon.

Subsystem	Design factor	Relation	Performance
Vehicle chassis	Speed	●	Vertical acceleration
	Mass		
	Damping coef.		
	Spring coef.		
	Geometric data		
Ammunition - Projectile - Propellant	Proj. mass	●	Max. range
	Prop. mas.		
	Drag coef.		
	Diameter		
	Length		
Gun Tube	Muzzle velocity	●	Rate of Fire (ROF)

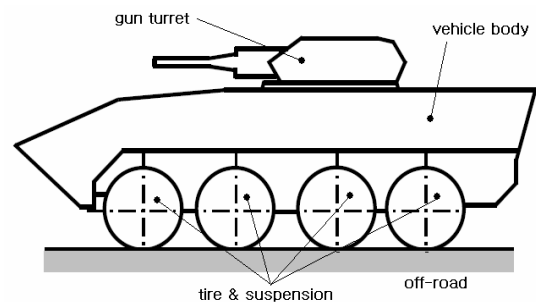


Fig. 2. A four-wheeled armored vehicle.

2.2 Mobility of wheeled armored vehicle

Fig. 2 represents a wheeled armored vehicle composed of a vehicle body, a gun turret, tires and mechanical suspension units. The overall performance of this ground weapon is judged by the firing power, and which is in turn strongly affected by the firing accuracy, the mobility and the physical properties. The current study is restricted to the enhancement of the mobility.

The shock stemming from the impulsive force at firing gives rise to the dynamic excitation to the driver's seat, after being transferred via the vehicle body which is being driven on the non-paved off-ground. The unstable oscillation of the vehicle body significantly affects the firing accuracy so that the time required for making the vehicle be in the stable state becomes a crucial factor determining the fighting power. The mobility is judged by the time spent for making the horizontally oscillating inclination angle of a wheeled armored vehicle be within 3° after firing a bullet, while passing over bumps at a constant speed.

The factor contributing the greatest effect on the mobility is known as the vehicle travelling speed, which is determined by the engine power and vibration in traveling as well as the shock characteristics. However, most vehicle engines are not permitted to be designed but chosen from the standards produced. From this reason, the stabilization time is mostly influenced by the suspension unit once a vehicle engine is chosen.

On the other hand, the detailed specifications of a wheeled

Table 2. Numerical parameters and initial design values taken for the half-car model.

Parameters	Symbols	Units	Values	Remarks
Vehicle speed	V	m/s	1.0	-
Suspended mass	m_s	kg	567.0	-
Pitching moment of inertia	I_s	$kg \cdot m^2$	600.0	-
Front and rear unsuspended masses	m_1, m_2	kg	72.5	-
Front and rear spring coefficients	K_1, K_2	kN/m	28,030	Design variable
Front and rear damping coefficients	C_1, C_2	$kN \cdot s/m$	3,000	Design variable
Front and rear tire spring coefficients	K_{T1}, K_{T2}	kN/m	400,000	Design variable
Front and rear tire damping coefficients	C_{T1}, C_{T2}	$kN \cdot s/m$	162	Design variable
Distance between front axle and center of gravity	a	m	0.9	-
Distance between rear axle and center of gravity	b	m	1.0	-
Bump radius	R_b	m	0.1	-

armored vehicle, such as vehicle size and weight, track, ground condition are not determined at the concept design stage. This makes the identification of input data and the synthesis of the simulation results difficult. Accordingly, the present study employs a half-car dynamic model to access the performance level of the suspension unit under consideration, at the concept design stage. The vertical acceleration of the vehicle body (equally, the driver's seat), which is exerted when the model passes through a single bump at a given constant speed without firing, is also taken as an additional quantity influencing the mobility. This is because the road-induced shock [16] transferred to the vehicle body characterizes the vertical absorption performance of the suspension unit, independently from the shock absorption against the horizontal impulsive shock at firing.

3. Approximation of the dynamic responses

In the current study, an optimization is performed for two individual subsidiary quantities, the stabilization time and the vertical acceleration, as well as the final mobility performance of a four-wheeled armored vehicle. The responses of the two subsidiary quantities to the design variables of the suspension unit are analyzed through a half-car dynamic mode and approximated by the 1st-order RSM method with the help of DOE. After that, the 2nd-order response surface method follows the fitness evaluation of the 1st-order response surfaces approximated. A stepwise regression is employed to improve the fitness of the approximated response surfaces.

3.1 Half-car dynamic model

Fig. 3. shows a half-car dynamic model of the four-wheeled armored vehicle under consideration, which consists of unsuspended, suspended and tires. Numerical parameters taken for this model are recorded in Table 2, where four parameters are chosen as the design variables. A half-car model is widely used to evaluate the basic kinetic behaviors of the concept designs of various kinds of vehicles. It is also employed to the

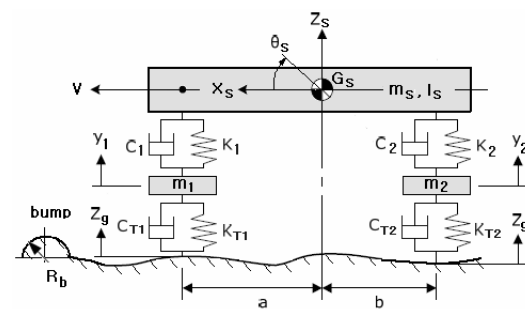


Fig. 3. A half-car dynamic model for the four-wheeled armored vehicle under consideration.

VEHDYN II [17] of the US army, a program to simulate the vehicle mobility.

The motion of the dynamic model is restricted to 2-D planar, and both the unsuspended and suspended are assumed to be rigid. Damped elastic properties of both suspension and tire [18, 19] are expressed in terms of the Voigt models, and the corresponding spring constants and damping ratios are set by variables to be tailored. Note that spring constants and damping ratios of front and rear parts are set equally such that the total design variables become four, $X_1 = K$, $X_2 = C$, $X_3 = K_T$ and $X_4 = C_T$.

Denoting $\mathbf{Y} = \{Z_s, \theta_s, y_1, y_2\}^T$, the dynamic response of the half-vehicle model shown in Fig. 3 is governed by

$$[\mathbf{M}]\ddot{\mathbf{Y}} + [\mathbf{C}]\dot{\mathbf{Y}} + [\mathbf{K}]\mathbf{Y} = \mathbf{F}(t) \quad (1)$$

with the mass, damping and stiffness matrices defined in Appendix A. While, the external load vector $\mathbf{F} = \{F_s, F_\theta, F_1, F_2\}^T$ is composed of F_s and F_θ stemming from the impulse at firing, and the road excitations $F_1 = K_{T1}Z_g$ and $F_2 = K_{T2}Z_g$. Note that we apply the impulsive force which is measured by experiment at the firing showing the longest firing distance is used.

A test Fortran program was coded to numerically solve the above dynamic equations, in which the fourth-order Runge-

Kutta method is employed. The reader may refer to the book by James et al. [20] for the detailed numerical solution procedure.

3.2 Design of experiments

A 2^k – type DOE is used to approximate the response surfaces of the stabilization time and vertical acceleration of the half-car dynamic model, in which the total number of experiments becomes 16 if the factor k is set by 4. But an additional experiment case is added to detect the curvature of the approximated surface, resulting in a total of 17 experiment cases, as given in Table 3. Where, 10% higher and lower than the initial design values recorded in Table 2 are taken for +1 and -1, respectively, while the initial design values are used for an additional experiment case (i.e., the 17th case) with the level (0,0,0,0).

Among 17 experiment cases, the 11th case with $X_{11} = \{-1, 1, -1, 1\}$ provides us the shortest stabilization time of 0.414 sec, while the 1st, 5th, 9th and 13th cases do the longest stabilization time of 0.567 sec. On the other hand, the 8th case produces the largest vertical acceleration of 2.704G, while both the 1st and 9th cases do the lowest value of 1.914G.

3.3 Response surface of the stabilization time

Using the experimental results, we performed the main effect analysis to find the relations between each design variables and the stabilization time. As represented in Fig. 4, one can find that the damping ratio of the suspension unit has the greatest effect on the stabilization time. The inherent effect of damping on the stabilization time can be easily found from various vibration systems, so that the response surface approximated for our half-car dynamic model represents the inherent physical behavior well.

Table 3. A L_{16+1} DOE table and the case experiment results.

Case	Orthogonal array L_{16+1} with an additional case				Stabilization time (sec)	Vertical acceleration (G)
1	-1	-1	-1	-1	0.567	1.914
2	+1	-1	-1	-1	0.513	1.931
3	-1	+1	-1	-1	0.414	2.232
4	+1	+1	-1	-1	0.468	2.245
5	-1	-1	+1	-1	0.567	2.306
6	+1	-1	+1	-1	0.513	2.326
7	-1	+1	+1	-1	0.420	2.688
8	+1	+1	+1	-1	0.462	2.704
9	-1	-1	-1	+1	0.567	1.914
10	+1	-1	-1	+1	0.513	1.928
11	-1	+1	-1	+1	0.414	2.240
12	+1	+1	-1	+1	0.468	2.253
13	-1	-1	+1	+1	0.567	2.301
14	+1	-1	+1	+1	0.513	2.322
15	-1	+1	+1	+1	0.420	2.695
16	+1	+1	+1	+1	0.462	2.711
17	0	0	0	0	0.519	2.295

Fig. 5 represents the variation of the stabilization time to each combination of two distinct design variables (that is, the bilinear 2-way interactions). Remarkable variations are observed in Figs. 5 (a), 5 (d) and 5 (e), confirming the significant influence of the suspension damping ratio once again.

We next estimate the effects of main, 2-, 3- and 4-way interactions of the design variables on the stabilization time, and the estimated results are recorded in Table 4. This is needed to determine how many terms should be included into the final response surface which satisfies the suitable approximation accuracy and to examine whether the further extension of design of experiments is needed. The analysis of variance is also applied to the estimated effects and coefficients of each source term which influence the stabilization time, and the estimated results are given in Table 5.

Referring to Table 5, both the main terms and the 2-way interactions exhibit the significant p-value of 0, while the 3-way and the 4-way interactions show the insignificant p-values of 0.762 and 0.674 respectively. In the 2-way interaction, the bilinear term $K \times C$ shows the highest effect equal to 0.0465, while the term $K \times K_T$ does not give the effect at all. According to the detailed numerical results, we found that R^2 is 0.98 but adj. R^2 is as low as 0.76. As well, we found that there exists a curvature effect p-value of 0.027, so it is judged that there exists a stationary point among the experimental points.

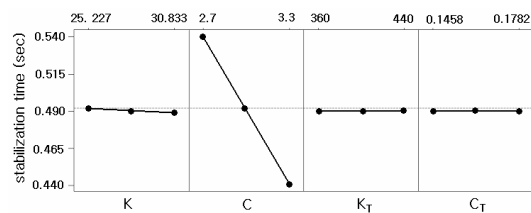


Fig. 4. Main effects of each design variables (linear terms) on the stabilization time.

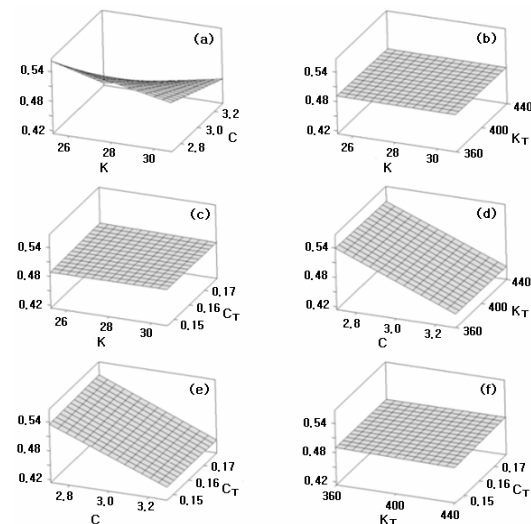


Fig. 5. Variations of the stabilizing time with respect to: (a) K and C , (b) K and K_T , (c) K and C_T , (d) C and K_T , (e) C and C_T , and (f) K_T and C_T .

Table 4. Estimated effects and coefficients of each term for approximating the stabilization time.

Term (Source)	Effect ($\times 10^{-3}$)	Coeff. ($\times 10^{-3}$)	t-value	p-value
Constant	-	489.55	189.18	0.000
X_1	1.50	-0.75	-0.29	0.779
X_2	-96.75	-48.37	-18.41	0.000
X_3	-2.25	-1.13	-0.43	0.674
X_4	2.25	1.12	0.43	0.674
$X_1 \times X_2$	46.50	23.25	8.85	0.674
$X_1 \times X_3$	-0.00	-0.00	-0.0	1.000
$X_1 \times X_4$	-2.25	-1.12	-0.43	1.000
$X_2 \times X_3$	0.75	0.37	0.14	0.674
$X_2 \times X_4$	-2.25	-1.13	-0.43	0.888
$X_3 \times X_4$	2.25	1.12	0.43	0.674
$X_1 \times X_2 \times X_3$	-6.00	-3.00	-1.14	0.269
$X_1 \times X_2 \times X_4$	2.25	1.13	0.43	0.674
$X_1 \times X_3 \times X_4$	-2.25	-1.13	-0.43	0.674
$X_2 \times X_3 \times X_4$	-2.25	-1.12	-0.43	0.674
$X_1 \times X_2 \times X_3 \times X_4$	2.25	1.12	0.43	0.674

* SE coefficients: 25.88×10^{-4} for all terms

Table 5. Estimation of the variation of the stabilization time.

Source	DF	Adj. SS ($\times 10^{-4}$)	Adj. MS ($\times 10^{-4}$)	t-value	p-value
Main	4	749.835	187.459	84.83	0.000
2-way	6	174.230	29.040	13.14	0.000
3-way	4	4.095	1.024	0.46	0.762
4-way	1	4.095	2.210	0.18	0.674
RE	17	37.567	1.912	-	-
CE	1	8.947	8.947	5.0	0.027
PE	16	28.620	1.789	-	-
Total	32	966.142	-	-	-

* Seq. SS = Adj. SS for all sources, RE: Residual Error, CE: Curvature Effect, PE: Pure Error

Therefore we exclude the 3-way and 4-way interactions which are not significant and consider only a constant, the linear terms and the 2-way interaction for estimating the effects of individual factors and coefficients. Thereafter, an analysis of variance is carried out. The lack of fit test shows the p-value of 0.77, the coefficient of determination R^2 of 0.98, and adj. R^2 of 0.96, which justifies that the fit of the response surface is acceptable for approximating the stabilization time. As a consequence, the equation of the response surface expressed in terms of a constant, main terms and 2-way interaction is given by

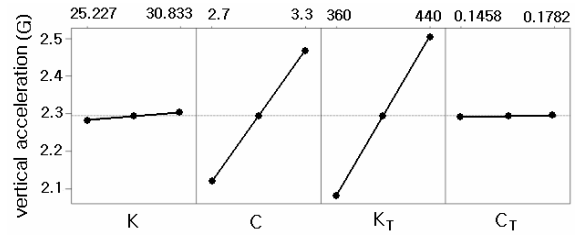


Fig. 6. Main effects of each design variables (linear terms) on the vertical acceleration.

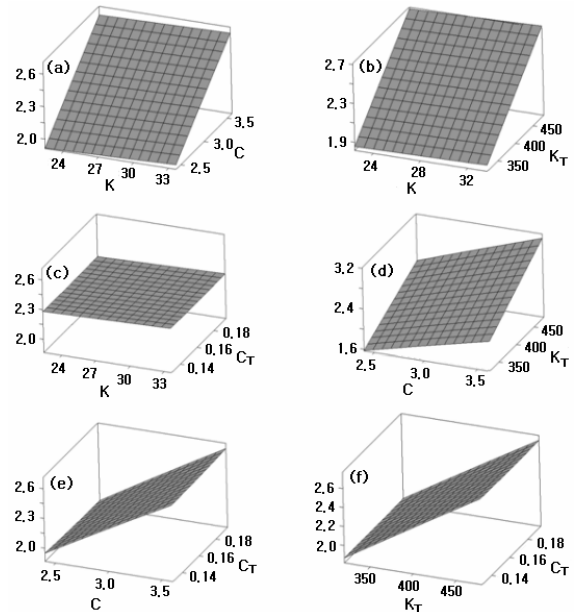


Fig. 7. Variations of the vertical acceleration with respect to: (a) K and C , (b) K and K_T , (c) K and C_T , (d) C and K_T , (e) C and C_T , and (f) K_T and C_T .

$$\begin{aligned}
 f_1(\mathbf{X}) = & 3.2308 - 0.0792009X_1 - 0.91125X_2 \\
 & - 0.00040312X_3 + 0.76389X_4 \\
 & + 0.0276489X_1X_2 - 0.0247750X_1X_4 \\
 & + 0.00003125X_2X_3 - 0.231481X_2X_4 \\
 & + 0.00173611X_3X_4
 \end{aligned} \tag{2}$$

3.4 Response surface of the vertical acceleration

Based on the experimental results given in Table 3 for the vertical acceleration using the 2^4 -type DOE with an additional experiment case, as explained in Section 3.2, a main effect analysis is carried out to examine the relations between the design variables and the vertical acceleration. As shown in Fig. 6, the design variables that give rise to the greatest effects on the vertical acceleration are found to be C and K_T .

The variation of the vertical acceleration to each combination of two distinct design variables (that is, the effects of the 2-way interactions) is represented in Fig. 7. The strong dependence of the vertical acceleration on C and K_T is apparent also in the bilinear response. The effects, coefficients, t- and p-values of the 16 terms are recorded in Table 6.

Table 6. Estimated effects and coefficients of each source term for approximating the vertical acceleration.

Term (Source)	Effect ($\times 10^{-3}$)	Coeff. ($\times 10^{-3}$)	t-value	p-value
Constant	-	2,294.41	16,000	0.000
X_1	16.25	8.12	53.60	0.012
X_2	353.25	176.62	1,165.19	0.001
X_3	424.50	212.25	1,400.21	0.000
X_4	2.25	1.12	7.42	0.085
$X_1 \times X_2$	-1.75	-0.88	-5.77	0.109
$X_1 \times X_3$	2.00	1.00	6.60	0.096
$X_1 \times X_4$	-0.25	-0.13	-0.82	0.561
$X_2 \times X_3$	32.50	16.25	107.20	0.006
$X_2 \times X_4$	5.25	2.62	17.32	0.037
$X_3 \times X_4$	-1.00	-0.50	-3.30	0.187
$X_1 \times X_2 \times X_3$	-0.50	0.25	-1.65	0.347
$X_1 \times X_2 \times X_4$	0.25	0.12	0.82	0.561
$X_1 \times X_3 \times X_4$	0.50	0.25	1.65	0.347
$X_2 \times X_3 \times X_4$	0.50	0.25	1.65	0.347
$X_1 \times X_2 \times X_3 \times X_4$	0.50	-0.25	-1.65	0.347

* SE coefficients: 1.47×10^{-4} for the constant and 1.52×10^{-4} for the other terms

Table 7. Estimation of the variation of the vertical acceleration.

Source	DF	Adj. SS ($\times 10^{-3}$)	Adj. MS ($\times 10^{-4}$)	t-value	p-value
Main	4	1,221.02	187.459	3,052.55	0.001
2-way	6	4.37	29.040	7.28	0.017
3-way	4	0.0	1.024	0.01	0.462
4-way	1	0.0	2.210	0.0	0.347
RE	1	0.0	1.912	0.0	-
CE	1	0.0	8.947	0.0	-
Total	16	1.225	-	-	-

* Seq. SS = Adj. SS for all sources, RE: Residual Error, CE: Curvature Effect, PE: Pure Error

As for the stabilization time, an analysis of variance is applied to the estimated effects and coefficients of 16 sources given in Table 6. The estimated results are presented in Table 7, where the 2-way interaction shows the significant p-value of 0.017. On the contrary, both the 3-way and 4-way interactions are found to be insignificant such that both exhibit p-values of 0.462 and 0.347, respectively. As well, we found that both R^2 and adj. R^2 reach almost 1.0.

However, since the 2-way interaction is significant, further experiment is performed, with an additional axial point, to estimate the effect of quadratic terms of individual design variable on the response surface. The analysis of variance is made with the coefficients estimated for each term, which are

calculated through the further case experiments. We found, from the detailed numerical results, that the quadratic terms give rise to the remarkable influence, as well as both the linear and 2-way interaction terms. So, we include four quadratic terms into the response surface approximation of the vertical acceleration, while excluding the 3- and 4-way interactions. The final approximated response surface in terms of a constant, main and 2-way interactions, and the four quadratic terms is given by

$$\begin{aligned}
 f_2(\mathbf{X}) = & 0.085 + 0.00160542X_1 + 0.0772222X_2 \\
 & + 0.00153125X_3 - 0.00104055X_1X_2 \\
 & + 0.000021213X_1^2 - 0.0148148X_2^2 \\
 & - 0.00000052083X_3^2 + 4.92176X_4^2 \\
 & - 2.75206X_4 + 0.00000891902X_1X_3 \\
 & - 0.00275278X_1X_4 + 0.00135417X_2X_3 \\
 & + 0.540123X_2X_4 - 0.000771605X_3X_4
 \end{aligned}
 \tag{3}$$

4. Optimization of vehicle mobility

The optimum design of the damping ratios and spring coefficients of the suspension unit including tires for maximizing the mobility of the model vehicle is formulated such that

$$\begin{aligned}
 \text{Find } & \mathbf{X} = \{X_1, X_2, X_3, X_4\} \\
 \text{Minimize } & F(\mathbf{X}) = w_1f_1(\mathbf{X}) + cw_2f_2(\mathbf{X}) \\
 \text{subject to } & \\
 & X_i \geq 0, \quad i = 1, 4 \\
 & 25.227 \leq X_1 \leq 30.833 \\
 & 2.7 \leq X_2 \leq 3.3 \\
 & 360 \leq X_3 \leq 440 \\
 & 0.1458 \leq X_4 \leq 0.1782
 \end{aligned}
 \tag{4}$$

with the weighting factors w_1 and w_2 and the scaling factor $c = |f_1|/|f_2|$.

The generalized optimization problem (4) may be transformed into an optimization problem for minimizing either the stabilization time or the vertical acceleration, depending on the choice of two weighting factors. So, in the current study we perform three separate optimization problems: (i) for minimizing the stabilization time ($w_2 = 0$), (ii) for minimizing the vertical acceleration ($w_2 = 0$), and (iii) for maximizing the mobility with the equal weights ($w_1 = w_2 = 0.5$). Note that the third case is not a multiobjective problem any longer, because the weights are not variable to be controlled but fixed. The PLBA (Pshenichy-Lim-Belegundu-Arora) algorithm, which is based on recursive quadratic programming, is used to seek the optimum solutions for each optimization problem.

The optimum solution of problem (i) is represented in Table 8, where the error denotes the relative difference to the solution obtained by plugging the four optimum design variables into the Eq. (1) of the half-dynamic model. Meanwhile, the

Table 8. Optimum solution of the stabilization time (ST).

	K	C	K_T	C_T	ST (sec)	Error (%)
Optimum solution	25,227	3,300	400,200	145,8	0.418	0.65
Solution (Eq. (1))	same	same	same	same	0.420	

Table 9. Optimum solution of the vertical acceleration (VA).

	K	C	K_T	C_T	VA (G)	Error (%)
Optimum solution	25,227	2,70	360,000	178,2	1.913	0.05
Solution (Eq. (1))	same	same	same	same	1.914	

Table 10. Optimum solution for maximizing the vehicle mobility.

	K	C	K_T	C_T	ST (sec)	VA (G)
Optimum solution	30,830	3,300	360,000	178,2	0.47	2.30
Solution (Eq. (1))	same	same	same	same	0.47	2.25

stabilization time obtained by the optimization is larger than the minimum value of 0.414 of the case experiments in Table 1. This is caused by the inherent difference between the actual response and the approximated response surface. However, the relative error is less than 1% so that the accuracy of the approximated response surface of the stabilization time, that is Eq. (2), has been justified.

The optimum solution of problem (ii) is given in Table 9, where the relative error with respect to the solution which is obtained by substituting the optimum design variables into Eq. (1) is extremely tiny. Furthermore, this value is smaller than the minimum vertical acceleration 1.914 among the case experiments. Thus the approximated response surface given by Eq. (3), which consider the quadratic terms of each design variable, is highly accurate.

The optimization results of problem (iii) for maximizing the vehicle mobility are represented in Table 10. To enhance the vehicle mobility, both the stabilization time and vertical acceleration should be reduced simultaneously. However, both performances exhibit a remarkable conflicting variation to the design variable, particularly to the suspension damping ratio C ; the two performances given in Table 10 are larger than those in Tables 8 and 9. Note that the optimization results in Table 10 vary depending on the choice of two weights w_1 and w_2 in Eq. (4).

The optimum solution given in Table 10 is nothing but a Pareto solution within the feasible regions formed by the four design variables, as illustrated in Figs. 8 and 9, when two weights w_1 and w_2 are set equally by 0.5. The choice of weights depends on not only the goal of optimization problem at hand but the designer's empirical intuition [21].

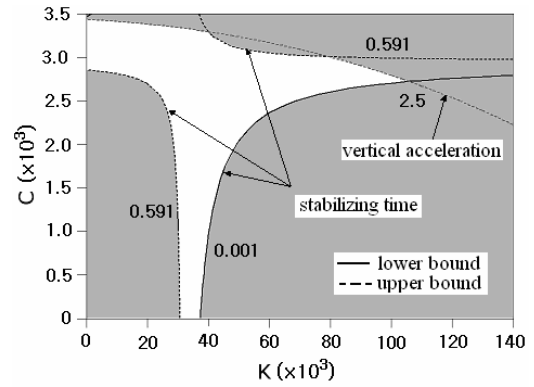


Fig. 8. Overlaid contour plot with respect to K and C .

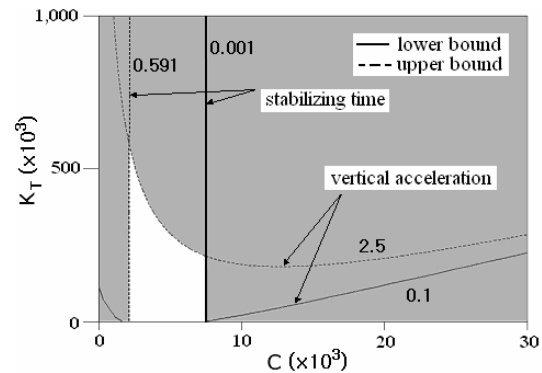


Fig. 9. Overlaid contour plot with respect to C and K_T .

5. Conclusion

An optimum design procedure for the suspension unit of a wheeled armored vehicle to maximize the mobility has been explored, by making use of a half-car dynamic analysis model, the response surface method, and the PLBA algorithm. The proposed optimization procedure has been fully validated and verified through illustrative numerical experiments.

From the case experiments using an extended orthogonal array, we found that the two subsidiary performances of the vehicle, the stabilization time and the vertical acceleration show remarkably conflicting variations to the suspension damping ratio. The two response surfaces approximating the stabilization time and the vertical acceleration have been justified to be highly accurate such that the relative approximation errors in the final optimum solutions are less than 1%. The objective function for the final mobility optimization was defined as a linear combination of the two subsidiary performances with equal weights. Due to the conflicting variation between the two subsidiary performances of the vehicle, the mobility optimization led to a stabilization time and a vertical acceleration larger than those obtained by the two single-objective optimizations.

References

[1] G. H. Hohl, Military Terrain vehicles, *Journal of Terramechanics*, 44 (2007) 23-34.

- [2] J. Y. Wong and W. Huang, Wheels vs. tracks – a fundamental evaluation from the traction perspective, *Journal of Terramechanics*, 43 (2006) 27-42.
- [3] A. Dhir and S. Sankar, Assessment of tracked vehicle suspension system using a validated computer simulation model, *Journal of Terramechanics*, 32 (3) (1995) 127-149.
- [4] S. Nell and J. L. Steyn, Development and experimental evaluation of translational semi-active dampers on a high mobility off-road vehicle, *Journal of Terramechanics*, 40 (2003) 25-32.
- [5] J. R. Cho, H. W. Lee, W. S. Yoo and J. K. Lee, Study on damping characteristics of hydropneumatic suspension unit of tracked vehicle, *KSME International Journal*, 18 (2) (2004) 262-271.
- [6] J. Yamakawa and K. Watanabe, A spatial motion analysis model of tracked vehicles with torsion bar type suspension, *Journal of Terramechanics*, 41 (2004) 113-126.
- [7] S. A. Shoop, P. W. Richmond and J. Lacombe, Overview of cold regions mobility modeling at CRREL, *Journal of Terramechanics*, 43 (2006) 1-26.
- [8] G. M. Bocheneck and J. Kim, *Advanced Collaborative Environments Supporting Systems Integration and Design*, RTO-MP-089-09, NATO (2002).
- [9] M. A. French and M. J. Lewis, *Demonstrating the Potential Use of Virtual Prototype Modeling Techniques for Future AFVs*, RTO-MP-089-08, NATO (2002).
- [10] B. Wiart, P. Peyronnet and Nicolas Moity, *SimEC3: Innovative Simulation Based Acquisition Tool for the France's Cooperative Fighting System*, RTO-MP-MSG-035-16, NATO (2002).
- [11] W. R. Krüger, O. Vaculin and W. Kortüm, *Multi-Disciplinary Simulation of Vehicle System Dynamics*, RTO-MP-089-16, NATO (2002).
- [12] R. H. Myers and D. C. Montgomery, *Response Surface Methodology-Process and Product Optimization using Designed Experiments*, Wiley, New York, (1995).
- [13] A. Todoroki and T. Ishikawa, Design of experiments for stacking sequence optimizations with genetic algorithm using response surface approximation, *Composite Structures*, 64 (3-4) 2004, 349-357.
- [14] O. K. Lim and J. S. Arora, An active set RQP algorithm for optimal design, *Computer Methods in Applied Mechanics and Engineering*, 57 (1986) 51-56.
- [15] *User's Manual: Army Weapon Effectiveness Analysis Model (AWAM)*, R.O.K Joint Chiefs of Staff, (2007).
- [16] J. R. Cho, K. W. Kim, D. H. Jeon and W. S. Yoo, Transient dynamic response analysis of 3-D patterned tire rolling over cleat, *European Journal of Mechanics A/Solids*, 24 (2005) 519-531.
- [17] D. C. Creighton, *Revised Vehicle Dynamics Module: User's Guide for Computer Program Vehdyn II*, Department of the Army, USA, (1985).
- [18] R. S. Sharp and D. A. Crolla, Road Vehicle Suspension System Design – Review, *Vehicle System Dynamics*, 16 (1987) 167-192.
- [19] R. K. Sleeper and R. C. Dreher, *Tire Stiffness and Damping Determined from Static and Free-vibration Tests*, NASA Technical Paper (1980).
- [20] M. L. James, G. M. Smith, J. C. Wolford and P. W. Whaley, *Vibration of Mechanical and Structural Systems: with Microcomputer Applications*, Harper Collins College Publishers, New York, (1994).



Eun-Ho Choi is currently a Ph.D. candidate at the Division of Mechanical System Design, Pusan National University. He received his B.S. in Mechanical engineering from Inje University in 2002, and M.S. in Mechanical Design Engineering from Pusan National University in 2004. His current research interests include structural optimization and multidisciplinary design optimization.



O-Kaung Lim received his B.S. in Mechanical Engineering from Seoul National University in 1972 and M.S. degree in Mechanical Engineering from KAIST in 1976, respectively. He then received his Ph.D. degree from the University of Iowa in 1982. He served as a head of the School of Mechanical Engineering in Pusan National University. Dr. Lim is currently a chair of the Education Committee of KSME. His current research interests include nonlinear optimization methods and programming.

Appendix A: Matrices in Eq. (1)

Three matrices in Eq. (1) are defined as follows:

$$[\mathbf{M}] = \begin{bmatrix} m_s & 0 & 0 & 0 \\ 0 & I_s & 0 & 0 \\ 0 & 0 & m_1 & 0 \\ 0 & 0 & 0 & m_2 \end{bmatrix} \quad (\text{A1})$$

$$[\mathbf{C}] = \begin{bmatrix} C_1 + C_2 & aC_1 - bC_2 & -C_1 & -C_2 \\ aC_1 - bC_2 & a^2C_1 + b^2C_2 & -aC_1 & bC_2 \\ -C_1 & -aC_1 & C_1 + C_{T1} & 0 \\ -C_2 & bC_2 & 0 & C_2 + C_{T2} \end{bmatrix} \quad (\text{A2})$$

$$[\mathbf{K}] = \begin{bmatrix} K_1 + K_2 & aK_1 - bK_2 & -K_1 & -K_2 \\ aK_1 - bK_2 & a^2K_1 + b^2K_2 & -aK_1 & bK_2 \\ -K_1 & -aK_1 & K_1 + K_{T1} & 0 \\ -K_2 & bK_2 & 0 & K_2 + K_{T2} \end{bmatrix} \quad (\text{A3})$$